Aberrometry explained

The design and use of the Zywave Aberrometer

Emma Deighan discusses the application of aberrometry in general ophthalmology

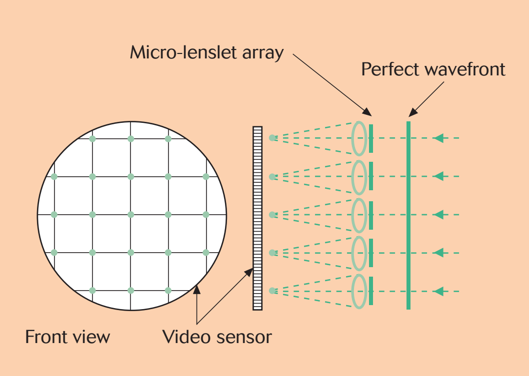

FIGURE 1. Principle of Hartmann-Schack aberrometry. A plane wavefront will hit the lenslet array perpendicular to the lens surface. This will produce an even distribution of centroids which correspond to the centres of each lenslet in the array

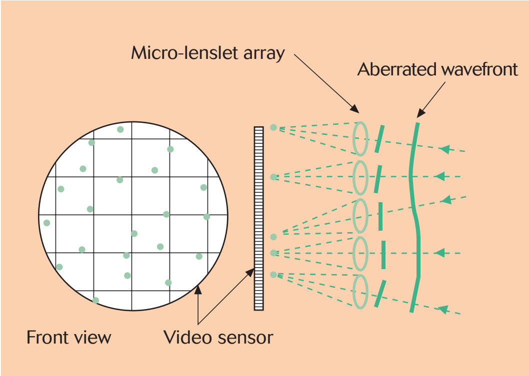

FIGURE 2. When the wavefront is not plane the angle of the wavefront at each lenslet causes displacement of the centroid from its expected position. The local slope of the wavefront at each lenslet determines the displacement of the centroid and so calculation can be employed to identify the local slope from the displacement. In this way total wavefront shape can be created

Laboratory-based aberrometry was developed into a clinical instrument in order to permit wavefront-guided laser vision corrections. However, these instruments are quickly finding an application outside refractive surgery in both general ophthalmology and contact lens practice.

The Zywave Aberrometer was launched by Bausch & Lomb in March 2000 as part of the Zyoptix customised ablation platform. Information from the Zywave aberrometer combined with data from the Orbscan II Z allows a personalised Zyoptix wavefront correction using the Technolas 217Z Excimer laser.

The Zywave quantifies aberrations throughout the entire optical system of the eye and in addition to spherical refraction, astigmatism and axis, can measure higher order aberrations. This gives a more comprehensive understanding of the patient's potential quality of vision that previously had been hard to quantify. It is interesting to note that the sum of the aberrations of each optical surface is less then the individual surface aberrations, suggesting that aberrations on one surface may be corrected by opposing aberrations on another.

HARTMANN SCHACK

The Zywave is based on the Hartmann Schack principle. A thin pencil of light is formed as a point focus on the retina and is then traced coming out of the eye until it passes through a lens array in the instrument.

If light is travelling in a parallel path (from a perfect optical system) it travels undeviated though the lens array as a plane wavefront. The light falls on the lenslet array perpendicular to the surface of the lenses. The focus of the individual points (centroids) is captured by a camera (CCD) and in a perfect optical system these points will form a grid with regular separation between the points (Figure 1).

In an aberrated optical system such as the eye, light will not exit the eye as a plane wavefront and so will not fall on the lenslet array perpendicular to the lens surfaces. The resulting image captured on the camera will demonstrate a distorted grid (Figure 2).

The direction and extent of the displacement of the centroids can be used to calculate the local slope of the wavefront as it hits the individual lenslet surfaces. The information from each centroid is then combined to give an overall measure of the wavefront aberration.

EFFECT ON VISION

Sphere and cylinder have the most significant impact on vision but the resulting wavefronts are simple in shape and relatively easy to correct by conventional means. However, the higher-order aberrations create much more complex wavefront patterns. While these may have lesser impact on gross vision than sphere and cylinder, their correction can improve quality of vision, especially in low light conditions. Higher-order aberrations become more pronounced towards the edge of the pupil and therefore have more significant impact on visual quality in low light conditions. When the pupil is constricted, aberrations are limited and the benefits of increased depth of field help overall visual quality. Since higher-order aberrations are more individual and far more complex than sphere and cylinder, they demand a much more personalised treatment plan.

Not all aberrations have the same impact on visual quality, depending on the complexity of the defocus created. Indeed, population data suggest that the average value is smaller and the variance between individuals decreases in the higher orders (fifth order and above), with

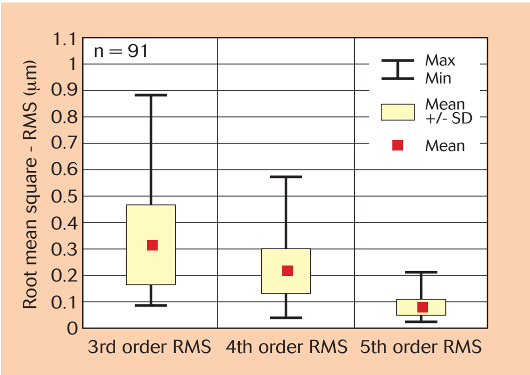

FIGURE 3. Distribution of higher-order aberrations in a normal population

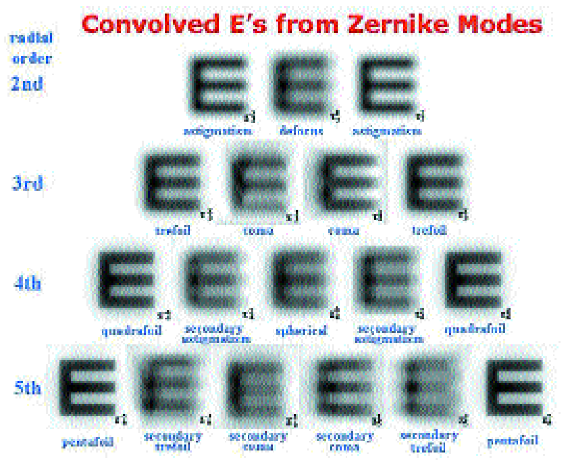

FIGURE 4. Predicted visual impact of various aberrations on vision

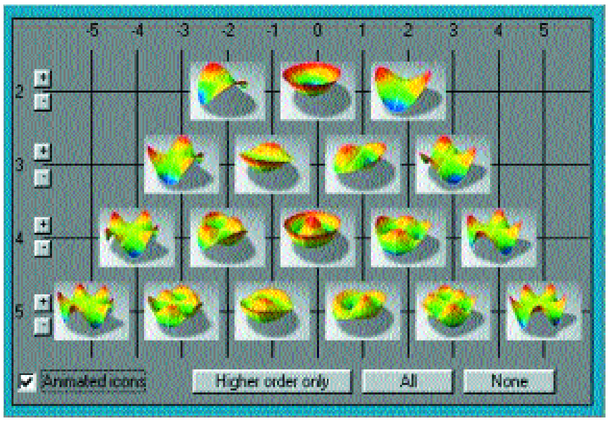

FIGURE 5. Wavefront shapes of the various Zernicke terms

lessening impact on visual quality (Figure 3). However, within orders and between orders, the exact visual impact varies with the type of aberration (Figure 4).

ZERNIKE POLYNOMIALS

Higher-order aberrations may be quantified in many ways. The Zywave aberrometer employs Zernike polynomials to do this. Zernike polynomials are mathematical expressions that define the type and extent of each of the wavefront aberrations. They are grouped into orders that define the complexity and type of aberration. Lower orders are simpler aberrations; for example, the second order includes defocus (sphere) and astigmatism, while higher orders are more complex, the fifth order including pentafoil and secondary coma (Figure 5).

A typical myopic wavefront is shaped like a bullet coming out of the eye (Figure 6), while a hyperopic wavefront is shaped like a bowl. These shapes define the relative position of the components of the wavefront. For the myopic eye the central part of the wavefront exits the eye in advance of the peripheral parts, the reverse being true for the hyperopic eye.

To analyse the wavefront further it is best to understand the different types of aberration and the unit of measure.

Second-order aber-

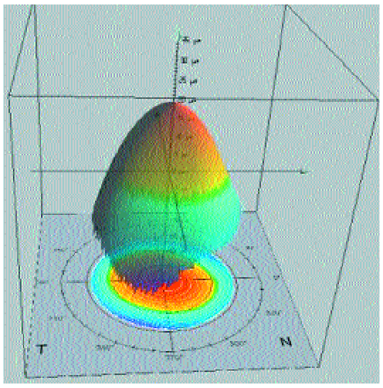

FIGURE 6. Typical wavefront shape of myopic defocus

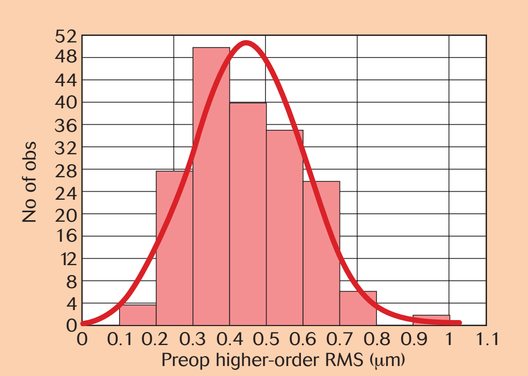

FIGURE 7. Distribution of higher-order aberration magnitude in the normal population

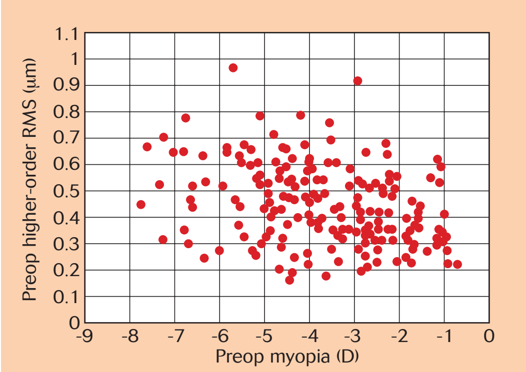

FIGURE 8. Correlation of higher-order aberrations with degree of ametropia showing that there is no correlation

rations include defocus and astigmatism (sphere and cylinder), the cylinder having two components relating to the two principal axes.

Defocus is symmetrical with a shape like a bowl, while astigmatism has the appearance of a Pringle crisp with the axes represented by the flat parts of the crisp.

Third order aberrations comprise coma and Trefoil which are the most common seen on the normal population.

Fourth-order aberrations comprise five components. There are two components each of quadrafoil and secondary astigmatism together with spherical aberration. This latter aberration is prevalent in patients complaining of night myopia since it has the effect of increasing the manifest myopia as the pupil dilates. It is also commonly induced during refractive surgery as a result of the transition between the flat, ablated area and the steeper peripheral cornea.

Fifth-order aberrations demonstrate much more complex wavefront shapes. However, they are usually present in lower degrees and consequently have less visual impact.

MEASUREMENT CAPABILITY

The ability of a Hartmann Shack aberrometer to measure higher order aberrations is linked to the spacing of the lenses in the lens array. As more lenslets are included with closer spacing between them, increasing orders of aberration can be measured.

However, as the number of lenslets is increased and the spacing reduced, the more likely the images from neighbouring lenslets are to cross over. This makes identifying the image from each lenslet more difficult and will cause difficulty in analysis, since the source of each image must be determined before an accurate estimate of wavefront aberrations can be made.

The Zywave measures up to and including the fifth order. The need for further complexity is called into question, given the population data which shows the lower incidence of aberrations beyond the fifth order and the minimal impact they would have on visual performance (Figure 3).

ROOT MEAN SQUARE

Wavefront aberration is measured in microns and each term can be individually measured. However, an overall estimate of higher order aberration can be obtained from root mean square (RMS) data. RMS calculation provides an average of all the Zernicke terms measured and reports them in microns. This can be assigned to account only for higher-order aberrations, excluding the defocus and astigmatism terms that can be corrected by conventional means.

Clinical experience suggests that a change of 0.1 microns is just visually detectable.

DISTRIBUTION OF ABERRATIONS IN THE NORMAL POPULATION

When examining the normal (pre-refractive surgery) population the RMS of higher order aberrations show that most patients display between 0.3 and 0.5 microns of aberration (Figure 7). This comprises mainly third- and fourth-order terms with only small degrees of fifth-order aberrations.

It is interesting to note that there is little relationship between degree of higher order aberrations and the amount of refractive error. High ametropes are no more likely to have higher order aberrations than the emmetrope (Figure 8).

Aberrations also increase towards the edge of the pupil and increasingly impact on visual quality as the pupil dilates (Figure 9). The Zywave reports the wavefront aberrations at a 6mm pupil size which is the standard suggested by the Optical Society of America. By following this standardisation, it allows easy comparison between patients both pre- and postoperatively as well as the outcomes of different methods of correction or different manufacturers products.

USING THE ZYWAVE ABERROMETER

The Zywave has been engineered to aid patient comfort and speed of acquisition. A new joystick combines easy height adjustment and control of image acquisi-

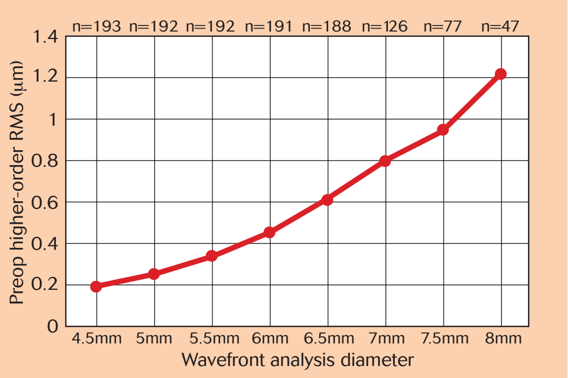

FIGURE 9. Change in higher-order aberrations with pupil size

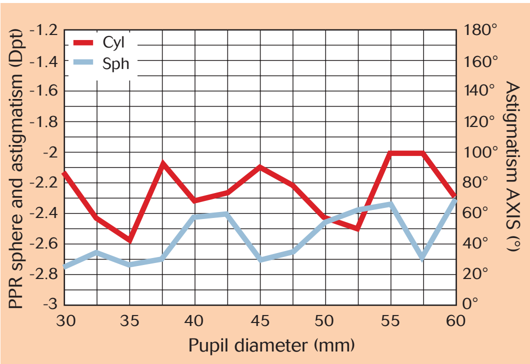

FIGURE 10. Change in predicted refraction with pupil size

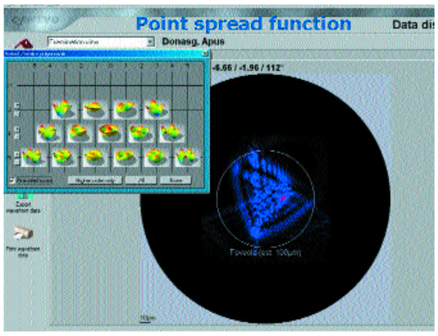

Figure 11. Point spread function (PSF) created from higher-order aberrations

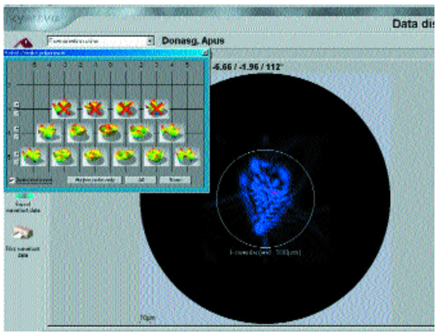
Figure 12. PSF showing effects of fourth and fifth order only


Figure 16. The Zyoptix Diagnostic Workstation

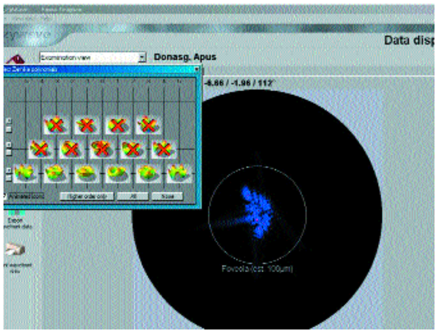
Figure 13. PSF showing effects of fifth order only

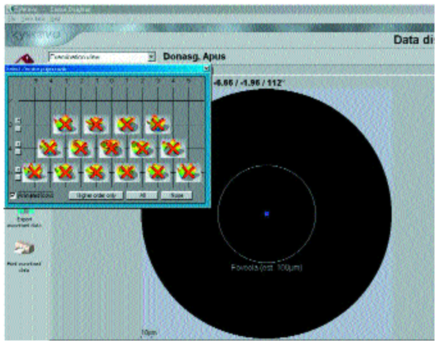
Figure 14. PSF showing diffraction limited effect (no higher order aberrations)

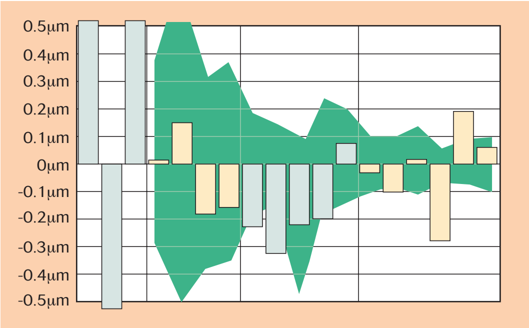

Figure 15. Patient aberrations plotted against normative data. Green bands show two standard deviations around the population mean

tion for the operator.

After the patient data have been entered and the patient correctly centred, the acquisition is started. The first step is to scan the eye to confirm correct imaging of the centroids on the CCD camera. The Zywave uses an automatic defocus to prevent patient accommodation. Once the centre of the pupil is confirmed sequential pictures are taken and automatically averaged. Once the measurement is taken, results can be interpreted using the different software features

ANALYSING WAVEFRONT MAPS

Colour maps show the aberration pattern for the whole wavefront (including sphere and cylinder) and for just the higher-order aberrations without sphere and cylinder.

These maps can also be viewed in 3-D mode to give a better understanding of the shape of the wavefront.

Predicted phoroptor refraction (PPR) readings are calculated to permit comparison between subjective (manifest) refraction and that derived from the wavefront analysis. The PPR calculates what the total refractive error would be at a predetermined pupil size which equates with that commonly found behind the phoroptor.

A PPR measurement is also given over the whole of the assessed pupil size and this reflects the influence of peripheral aberrations on overall refractive error. This concept can be understood more readily by considering the change in refraction across the pupil (Figure 10). The left vertical axis of the graph represents the amount of sphere or cylinder in dioptres. The right vertical axis indicates the direction of astigmatism. The horizontal axis shows the pupil size from 3mm up to the size of the pupil at the time of measurement.

A patient demonstrating consistent sphere and cylinder across a range of pupil sizes will usually correct well by conventional means. However, a patient that has a great variance in sphere and cylinder with increasing pupil size may report visual problems as the pupil size increases. While this may not be evident with high contrast charts in normal testing conditions, low light and low contrast charts may demonstrate the problem.

The presentation of the wavefront data may also be very useful to analyse patients with night vision problems following refractive surgery.

Another insight to the impact of aberrations on visual quality can be gained from an analysis of the pattern a distant point object forms on the retina, taking into account the various aberrations. A point spread function (PSF) can be used and analysed taking into account only the higher order aberrations.

Using the Zywave software it is possible to look at the effect of detected higher-order aberrations on the point spread function. (Figures 11-14). As each higher-order aberration is removed, the quality of the PSF improves until it reaches the diffraction-limited ideal.

Having collected normative data from the population, the Zywave is able to compare the specific aberrations in one patient to the normal population. The green band represents two standard deviations from normal (Figure 15). This helps the practitioner to determine the significance of the aberrations found.

Difference maps are another useful feature, where maps for the same patient can be subtracted from one and other to show the development over time.

The Zywave provides the practitioner with a greater understanding of potential visual quality and the contribution of higher-order aberrations, which has previously been hard to quantify.

There are currently over 320 Zywave Aberrometers in use worldwide and over 25,000 patients have undergone Zyoptix customised ablation procedures globally. Figure 16 shows the Zyoptix Diagnostic Workstation comprising the Zywave Aberrometer and the Orbscan IIZ.

Further Reading

Guirao, A, J Porter, D R Williams, and I G Cox, Calculated impact of higher order monochromatic aberrations on retinal image quality in a population of human eyes. *J Opt Soc Am A Opt Image Sci Vis*, 2002; 19(3): p. 620-8.

Williams, D, G Y Yoon, J Porter, A Guirao, H Hofer, and I Cox, Visual benefit of correcting higher order aberrations of the eye. *J Refract Surg*, 2000; 16(5): p. S554-9.

Guirao, A and D R Williams, A method to predict refractive errors from wave aberration data. *Optom Vis Sci*, 2003; 80(1): p. 36-42.

◆ *Emma Deighan is a DO and an application specialist for Bausch & Lomb UK*